Numerical analysis of in situ S-wave measurements

L'analyse numérique des mesures in-situ de propagation des ondes de cisaillement

C.MANCUSO, Istituto di Tecnica delle Fondazioni e Costruzioni in Terra (Geotecnica), Università di Napoli, Italy
A.L.SIMONELLI, Istituto di Tecnica delle Fondazioni e Costruzioni in Terra (Geotecnica), Università di Napoli, Italy
F.VINALE, Istituto di Tecnica delle Fondazioni e Costruzioni in Terra (Geotecnica), Università di Napoli, Italy

SYNOPSIS: This paper refers about recent developments in interpretation criteria of cross-hole measurements with reference to a field investigation carried out in a testing site in Fucino Valley (Italy). The subsoil consists of soft saturated lacustrine silty clays. A marked spreading phenomenon was generally observed and it was found that cross-correlation and group velocity are the most significant analysis techniques for determining the soil S-wave velocity.

1. INTRODUCTION

In situ measurement of propagation characteristics of artificially generated seismic waves represents, today, the most powerful tool for studying dynamic soil properties at very low strains ($<10^{-3} \div 10^{-4}$%). As a matter of fact, recorded signals contain all the necessary information concerning the deformability properties of sampled subsoil.

Unfortunately, in spite of the widespread use of field techniques, such as cross-hole and down-hole, interpretation procedures are often too simple, usually based on the identification of the wave arrival times at points spaced at certain distances from the source.

This paper refers about recent developments in interpreting criteria of Cross-Hole (CH) measurement with reference to an investigation carried out in a testing site in the Fucino Valley (Italy). The valley is a depression, 15 km in diameter, occupied since late Pleistocene by a lake where more than 100 m of fine grained soil deposited.

The subsoil consists of soft saturated lacustrine silty clays, with frequent organic matter, apparently uniform and without relevant macrostructural characteristics. The average index properties (D'Elia & Grisolia 1974) are: w_L = 80÷100%, I_P = 50÷60%, w = 70÷90%. At some depths, where organic levels are frequent, the clay presents higher values of w_L (>120%) and w (>100%).

The cross-hole tests were performed up to 40 m, using five bore-holes, spaced 5 m apart on the surface, along two ortogonal directions. For each bore-hole PVC casing was used and was grouted in place. Inclinometric measurements were performed to determine the actual spacing between receivers with depth: borehole deviations increase versus depth reaching at the bottom maximum values varying from 40 to 200 cm.

The tests were performed every 1.5 m; the data, acquired in digital form, were interpreted using either traditional or more recent numerical techniques.

2. NUMERICAL ANALYSIS TECHNIQUE REVIEW

Hereafter some numerical analysis techniques, based on digital acquisition of signals generated by the same impulse and recorded at two spaced receiving points, are briefly reported.

The **cross-correlation** $CC_{yx}(\tau)$ function gives a measure of the correlation degree of two signals, X(t) and Y(t), versus the time shift τ imposed to the traces. The analytical expression of cross-correlation is:

$$CC_{yx}(\tau) = \lim_{T\to\infty} \frac{1}{T} \int_T X(t)\cdot Y(t+\tau)\, dt \qquad (1)$$

where T is the length of the time record.

Most of the numerical analysis techniques operate in the frequency domain. Their use requires the decomposing of the time domain record into a group of harmonic waves of known frequency and amplitude. The algorithm used for this purpose is the well known Fast Fourier Transform (FFT).

In this way the cross-correlation can be rapidly calculated as:

$$CC_{yx}(\tau) = IFFT\,[G_{yx}(f)] \qquad (2)$$

where IFFT indicates the inverse fast Fourier transform and $G_{yx}(f)$ is the cross power spectrum defined below.

The **cross power spectrum** $G_{yx}(f)$ is a function of signals X(t) and Y(t), and is calculated as the product of the linear spectrum (L_x) of X(t) versus the complex coniugate (L_y^*) of the spectrum of Y(t):

$$G_{yx}(f) = L_x(f) \cdot L_y^*(f) \qquad (3)$$

For each frequency the cross power spectrum (CPS) is a vector in the complex field; its magnitudo and phase are respectively the product of the amplitude and the phase difference of the components of the two signals at that fixed frequency.

From the CPS **phase** $\Phi(f)$ it is possible to determine the apparent velocity («phase velocity») for each frequency component:

$$V(f) = L/T = L\cdot f = 2\cdot\pi\cdot f\cdot\frac{D}{\Phi(f)} \qquad (4)$$

where L is the wavelength, D is the distance between the receivers and Φ is in radiants.

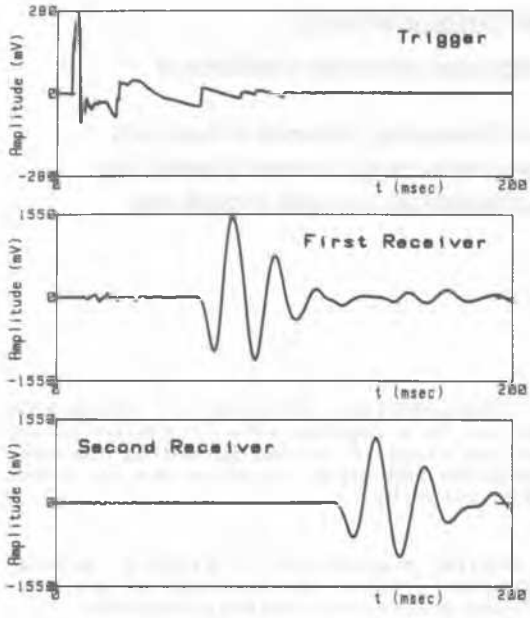

Figure 1. Example of time records (depth: 6 m).

From the **magnitudo M(f)** of the CPS it is possible to individuate the range of frequency components common to both signals.

As a matter of fact, field data are usually affected by noise; consequently it is a common practice to acquire and average several signals (at the same depth) with the aim of reducing the amount of noise. A measure of frequencies and amplitudes of noise is given by the **coherence** function $CO_{yx}(f)$, defined as follows:

$$CO_{yx}(f) = [\bar{G}_{yx}(f)\cdot\bar{G}_{xy}(f)]/[\bar{G}_{xx}(f)\cdot\bar{G}_{yy}(f)] \qquad (5)$$

where $(\bar{\ })$ indicates the averaging process.
In fact, the signal to noise ratio (S/N) is given by:

$$S/N\ (f) = CO_{yx}(f)/[1-CO_{yx}(f)] \qquad (6)$$

Therefore, CPS magnitudo and coherence permit the individuating of the frequency range common to both signals and not significantly affected by noise. Hence, it is possible to correctly interpret the phase $\Phi(f)$ (and phase velocity) of the averaged data.

3. TESTING SITE MEASUREMENT ANALYSIS

3.1 Visual analysis

The visual analysis consists, as well known, in the individuation of the characteristic points of the signals, hence in the determination of wave travel times.

An example of the time records obtained at the Fucino site is given in Figure 1, with reference to a depth of 6 m. The trigger record at source (S) allows to recognize the wave starting time (which is necessary to estimate direct travel times). The records at the receiver points (R1 and R2) allow to recognize the initial arrival times of the waves and hence to determine the direct velocities on paths S-R1 and S-R2 (V_{S-R1} and V_{S-R2}) and the interval velocity on path R1-R2 (V_0). From receiver records it is also possible to recognize other characteristic wave points, as peaks and troughs, and hence other interval velocities (V_1, ..., V_n).

At the testing site, difficulties sometimes arised in the visual interpretation of the field measurements because of the near-field effect (Sanchez-Salinero et al. 1986). In fact, at some depths a low predominant frequency of the signals is associated with low shear wave velocity, determining wavelengths comparable to the distance between the source and the first receiver; hence on the waveform recorded at the first receiver some near-field disturbance obscures the shear wave arrival.

The comparison of time records at the first and second receiver frequently shows a marked spreading phenomenon: during propagation the waveform changes its shape, increasing the time distances between peaks and troughs. This is due to the fact that, in a dissipative medium, as waves spread away from the source, their higher frequency components undergo a greater amplitude reduction because of their lower wavelenghts.

Spreading can also be recognized by the receivers' linear spectra (Figure 2), because the second receiver shows a marked reduction of higher frequency component amplitudes.

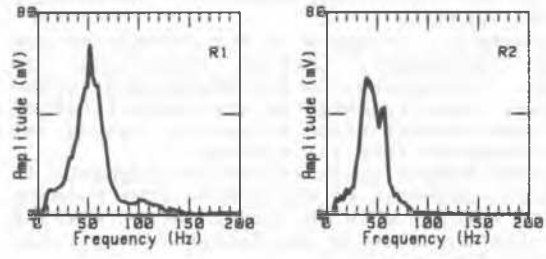

Figure 2. Linear spectra at 1st and 2nd receiver.

As an example, from the records in figure 1, the following decreasing wave velocity values were found: V_0= 84.6; V_1= 82.1; V_2= 80.1; V_3= 78.9; V_4= 77.0; V_5= 75.2 m/s.

The spreading phenomenon in the upper 20 m is shown in Figure 3, where the travel times, derived from the 1st to the 4th characteristic points, are reported.

The effect of spreading on low strain shear modulus G_{max} ($\propto V_s^2$) is even more important; for the measurement reported in figure 1, the difference between $G_{max}(V_0)$ and $G_{max}(V_1)$ is greater than 10% of $G_{max}(V_0)$, and reaches the 21% for $G_{max}(V_5)$.

With reference to this matter, theoretical studies on an ideal medium (Mancuso & Vinale 1988) demonstrated that the arrival time of S-waves is often recognizable with difficulty. Therefore, it was suggested to evaluate interval travel times looking at the characteristic points of the waveforms. However, if in an ideal medium the selection of the reference point is not effective on velocity values, in a real soil the selection is a problem of concern, as shown above.

The data interpretation obtained through recent numerical analysis techniques can provide useful solutions to this problem.

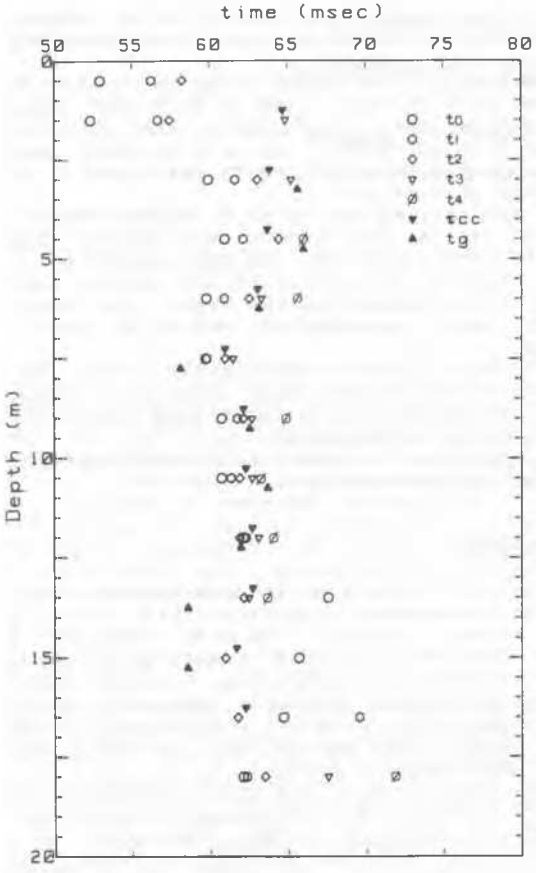

Figure 3. Spreading effects.

3.2 Numerical analysis

Field data have always been analysed using the cross-correlation technique. The interval travel time is equal to the shift time (τ_{cc}) corrisponding to the maximum of equation (1), or to the minimum if signals are opposite in polarity.

Figure 4 shows the CC of the time records presented in figure 1. The values are normalized by the maximum absolute value (CC_{max}).

Wave velocity is calculated as:

$$V_{cc} = D/\tau_{cc} \qquad (7)$$

where D is the distance between the receivers.

From a physical point of view, τ_{cc} represents the propagation time of the whole waveform travelling between the receivers. Hence, when a marked spreading is present and different velocity values arise, cross-correlation represents

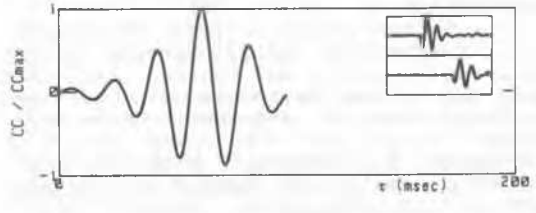

Figure 4. Example of Cross-Correlation.

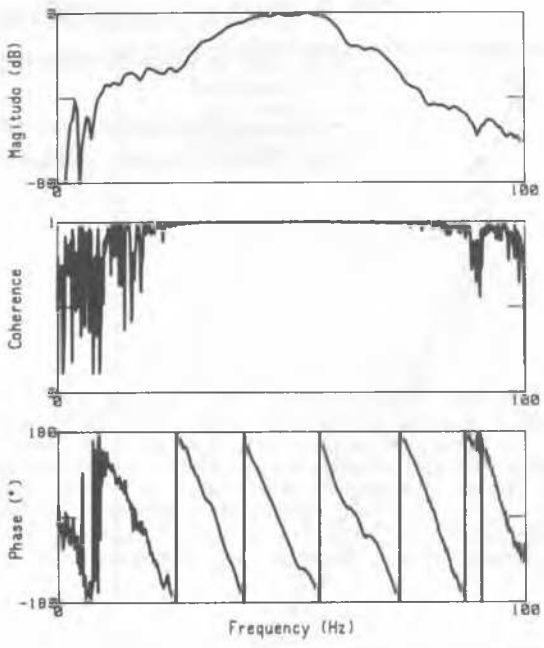

Figure 5. Magnitudo, Coherence and Phase.

a good, even if conventional, tool for characterizing the soil wave velocity.

Another technique, which was systematically used, is based on CPS and coherence of a series of signals generated at the same depth.

As explained in chapter 2, these functions allow to individuate the undisturbed frequency range of the signals. As an example, the CPS and coherence of the records obtained at 6 m of depth (Figure 5), indicate a significant frequency range of ≈20÷85 Hz.

After having selected the frequency components, a group travel time (t_g) can finally be defined by linearly interpolating the absolute CPS phase diagram (Bodare & Massarsch 1984):

$$t_g = \alpha/2\pi \qquad (8)$$

where α is slope of the line (Figure 6).

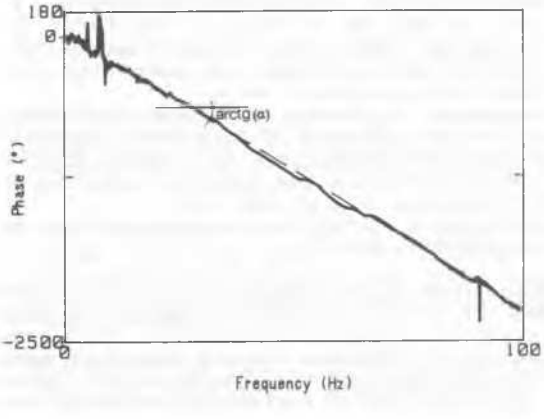

Figure 6. Linear interpolation of CPS phase.

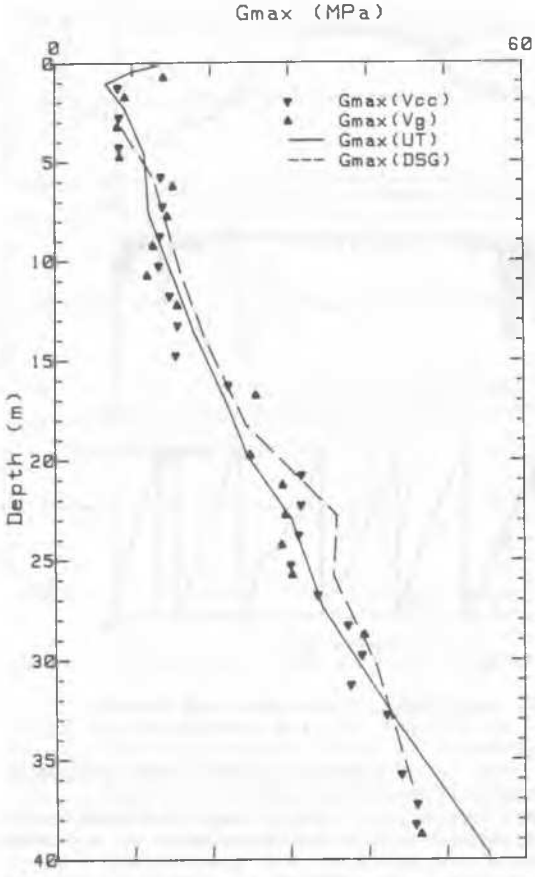

Figure 7. G_{max} moduli from CH, SASW and RC.

The velocity:

$$V_g = D/t_g \qquad (9)$$

obviously represents the propagation of the group of selected frequency components («group velocity»).

The two numerical techniques used to analyse the data gave similar results. For instance, with reference to the example reported in this paper, the following velocity values were determined (Figures 4 & 6): V_g=79.5 m/s; V_{cc}=79.6 m/s.

The cross-correlation and group velocity travel times within the first 20 m are compared in figure 3, as well as in Figure 7 (in terms of G_{max}); it can be noted that, at each depth, the results are in good agreement and generally lay within the visual analysis values.

In conclusion, although CC velocity and group velocity are the outcomes of different acquisition and analysis techniques, it clearly appears that they characterize the overall velocity of the whole waveform in a proper way.

For this reason, their use is suggested for determining material velocity.

At Fucino testing site several research groups have been involved in a project promoted by ENEA (Ente Nazionale Energie Alternative). This project consists in effectuating and comparing most of the traditional and new investigation techniques, with the aim of individuating static and dynamic soil properties as well as the relationships among them.

Some of the results are suited for a comparison with the G_{max} values derived from cross-hole tests, presented herein.

In particular, in figure 7 the CH results are compared with the ones from in situ SASW (Nazarian & Stokoe 1984), performed by the University of Texas (UT) and ISMES, as well as with those from Resonant Column (RC) tests performed at the University of Rome (DSG).

SASW was carried out up to a maximum depth of about 45 m. As well known, the sampled soil volume is much wider than the one sampled by CH method; however, on account of the lateral homogeneity of the subsoil in the area, the results of SASW (still unpublished) and of CH can be compared.

The RC tests (Pane & Burghignoli 1988) were performed on twelve specimens carefully sampled at several depths. Some tests give the profile of G_{max} modulus versus depth.

The comparison indicates an overall agreement among the various results.

4. CONCLUSIONS

An extensive CH investigation was carried out on the soft saturated lacustrine silty clays of Fucino Valley (Italy). The data acquired in digital form were analysed through both visual and recent numerical techniques. A marked spreading phenomenon was generally observed during wave propagation, causing significant differences among visual velocities, derived from signal characteristic points.

It was found that CC and group velocity are the most significant techniques to characterize the soil in terms of S-wave velocity. As a matter of fact, the two analysing methods, altough conceptually different, gave similar results.

These findings suggest an extensive use of the numerical analyses previously discussed, therefore encouraging further studies.

REFERENCES

Bodare, A. & Massarsch, K.R. (1984). Determination of shear wave velocity by different Cross-Hole methods. Proc. 8th WCEE, vol.III, 39-45, S. Francisco.

D'Elia, B. & Grisolia, M. (1974). On the behaviour of a partially floating foundation on normally consolidated silty clays. Proc. Symposium on settlement of structure, 91-98, Cambridge.

Mancuso, C. & Vinale, F. (1988). Propagazione delle onde sismiche: teoria e misura in sito. Atti del Convegno del Gruppo Nazionale di Coordinamento per gli Studi di Ingegneria Geotecnica, Monselice.

Nazarian, S. & Stokoe II, K.H. (1984). In situ shear wave velocities from spectral analysis of surface waves. Proc. 8th WCEE, vol.III, 31-38, S. Francisco.

Pane, V. & Burghignoli, A. (1988). Determinazione in laboratorio delle caratteristiche dinamiche delle argille del Fucino. Atti del Convegno del Gruppo Nazionale di Coordinamento per gli Studi di Ingegneria Geotecnica, Monselice.

Sanchez-Salinero, I., Roesset, J.M. & Stokoe II, K.H. (1986). Analytical studies of body wave propagation and attenuation. Report GR86-15, University of Texas, Austin.